



Screening of Lipid Composition for Scalable Fabrication of Solvent-Free Lipid Microarrays

Lida Ghazanfari and Steven Lenhart*

Department of Biological Sciences, Integrative NanoScience Institute, Florida State University, Tallahassee, FL, USA

Liquid microdroplet arrays on surfaces are a promising approach to the miniaturization of laboratory processes such as high-throughput screening. The fluid nature of these droplets poses unique challenges and opportunities in their fabrication and application, particularly for the scalable integration of multiple materials over large areas and immersion into cell culture solution. Here, we use pin spotting and nanointaglio printing to screen a library of lipids and their mixtures for their compatibility with these fabrication processes, as well as stability upon immersion into aqueous solution. More than 200 combinations of natural and synthetic oils composed of fatty acids, triglycerides, and hydrocarbons were tested for their pin-spotting and nanointaglio print quality and their ability to contain the fluorescent compound tetramethylrhodamine B isothiocyanate (TRITC) upon immersion in water. A combination of castor oil and hexanoic acid at the ratio of 1:1 (w/w) was found optimal for producing reproducible patterns that are stable upon immersion into water. This method is capable of large-scale nanomaterials integration.

Keywords: high-throughput screening, droplet microarray, lipid, lipophilic drug, nanointaglio

OPEN ACCESS

Edited by:

Jian Zhong,
Shanghai Ocean University, China

Reviewed by:

Barbara Sanavio,
Fondazione IRCCS Istituto
Neurologico Carlo Besta, Italy
Sílvia Castro Coelho,
Faculdade de Engenharia da
Universidade do Porto, Portugal

*Correspondence:

Steven Lenhart
lenhart@bio.fsu.edu

Specialty section:

This article was submitted to
Nanobiotechnology,
a section of the journal
Frontiers in Materials

Received: 09 June 2016

Accepted: 02 December 2016

Published: 23 December 2016

Citation:

Ghazanfari L and Lenhart S (2016)
Screening of Lipid Composition for
Scalable Fabrication of Solvent-Free
Lipid Microarrays.
Front. Mater. 3:55.
doi: 10.3389/fmats.2016.00055

INTRODUCTION

A fundamental goal of nanotechnology is to integrate top-down nanofabrication processes with bottom-up chemical assembly to reliably fabricate larger, more complex devices with molecular scale components (Rohrer, 1996). Liquid microdroplet arrays on surfaces are a promising approach toward achieving this goal by allowing multiple solutions to be integrated on a chip (Gosalia and Diamond, 2003; Popova et al., 2016). In principle, each droplet can be viewed as a microscopic test tube, allowing a density of containers limited only by droplet size and the ability to place different reagents into each droplet. For instance, an array with one droplet per square micrometer would allow 100 million containers on 1 cm² surface. The potential in high-throughput screening (HTS), with the state of the art being 10–30 wells/cm, is comparable to the difference in capabilities between early vacuum tube-based computer mainframes and today's solid-state computers.

Modern HTS requires robotics, liquid-handling devices, sensitive detectors, and software for data processing and control in order to perform millions of pharmacological tests on samples in parallel. Current robotic systems are burdened by several issues, such as high costs, poor reliability of data, standardization of data types, rapid and accurate dispensing of very small liquid volumes, and uncontrolled evaporation of dispensed liquids from Comley (2006). One promising approach to miniaturization of HTS is microfluidics. Microfluidic systems enable serial processing and analysis and, furthermore, can accomplish massive parallelization through

efficient miniaturization and multiplexing (Hong et al., 2009). In particular, droplet microfluidics use small droplets, typically water suspended in oil, to confine reagents and/or cells (Anna et al., 2003; Kim et al., 2015). A challenge in this field is that the droplets move and mix in solution, and a chemical tracker is therefore typically included in the drop for identification. Droplet microarrays provide a different solution to this technical challenge by attaching the droplet to a surface, so that its composition is known by its position in the array, at the cost of limiting the array to two dimensions (Gosalia and Diamond, 2003; Mugherli et al., 2009; Arrabito et al., 2013; Sun et al., 2015; Popova et al., 2016).

Microarrays of covalently attached monolayers are well established and allow the simultaneous analysis of thousands of chemical entities within a single experimental step (Cahill, 2001; Heller, 2002; Pirrung, 2002; Howbrook et al., 2003; Hook et al., 2006; Ma and Horiuchi, 2006). Biomolecules commonly immobilized on microarrays include proteins (Cahill, 2001), oligonucleotides (Heller, 2002; Pirrung, 2002; Howbrook et al., 2003), polymerase chain reaction products (Heller, 2002; Pirrung, 2002), peptides (Cahill, 2001; Howbrook et al., 2003), lipids (Howbrook et al., 2003; Hook et al., 2006), and carbohydrates (Ma and Horiuchi, 2006). Covalent small molecule microarrays are useful for screening for interactions with the surfaces of adherent cells. However, targets inside of the cell are inaccessible to this approach. Alternatives include embedding the small molecules into a matrix such as a hydrogel and allowing them to diffuse out (Bailey et al., 2004), a sandwich assay composed of microwells that are addressable by individual posts (Wu et al., 2011), or by generating arrays of microscopic water droplets for cell culture (Popova et al., 2016). These methods are promising for water-soluble compounds. However, an estimated 40% of approved drugs in the market and nearly 90% of molecules in the developmental pipeline are poorly water soluble (Kalepu and Nekkanti, 2015). This poses a challenge for delivery to cells through aqueous solution. We use lipid multilayer (or droplet) microarrays to temporarily immobilize lipophilic compounds onto a surface, allowing cellular uptake and quantitative dose-response curves (Kusi-Appiah et al., 2012; Kusi-Appiah et al., 2015). A crucial property of lipid multilayer microarrays for drug screening applications is that the layer must be thicker than a single monolayer or bilayer in order to contain enough drug to reach biologically relevant dosages upon cellular uptake.

Lipid multilayer microarrays have been fabricated by dip pen nanolithography (Lenhert et al., 2007), polymer pen lithography (Hirtz et al., 2015), nanointaglio printing (Lowry et al., 2014), and evaporative edge lithography (Vafai et al., 2015). Here, we use nanointaglio printing, which is a printing mode where ink is transferred from the recesses of a stamp, allowing for control of lipid multilayer film thicknesses by the stamp dimensions as well as the amount of ink on the stamp (Nafday et al., 2012). We have previously demonstrated that three different lipids can be integrated over larger areas by pin spotting of lipid solutions onto a palette, which is subsequently used to ink the intaglio stamp (Lowry et al., 2014). In order to scale this process up for integration of thousands of different lipid encapsulated drug candidates

for HTS, several obstacles must be overcome. First of all, we have previously used liposomal solutions in water for the microarray process, yet solvent evaporation becomes an issue as more compounds are added. Second, immersion of the lipid microarrays into water poses a challenge, as the lipids can sometimes be swept away upon addition of aqueous solution. In order to solve these problems, we here screen different fluid lipid carriers as a suitable matrix for solvent-free microarraying followed by intaglio printing and immersion into water. Our main objective here is to identify a fluid lipid composition capable of containing lipophilic small molecules and compatible with pin spotting and microarraying so that this process can be scaled up for HTS applications (Figure 1).

MATERIALS AND METHODS

Components

As shown in Figure 2, the components of the lipid formulations screened here include fatty acids [octanoic (caprylic) acid, hexanoic (caproic) acid, oleic acid, linoleic acid], triglycerols (olive oil, soybean oil, sesame oil, peanut oil, linseed oil, corn oil, cottonseed oil, castor oil, lavender oil, mineral oil, sunflower oil, safflower oil, canola oil, fish oil)/hydrocarbon (hexadecane), glycerol,

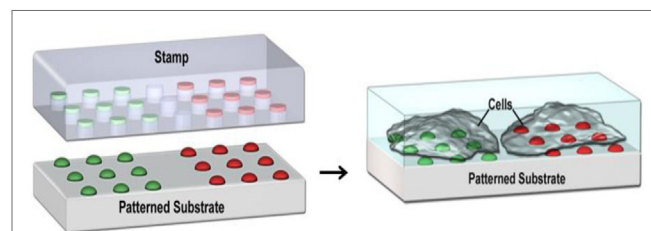


FIGURE 1 | Schematic showing the nanointaglio fabrication process (left) and its application in cell-based high-throughput screening.

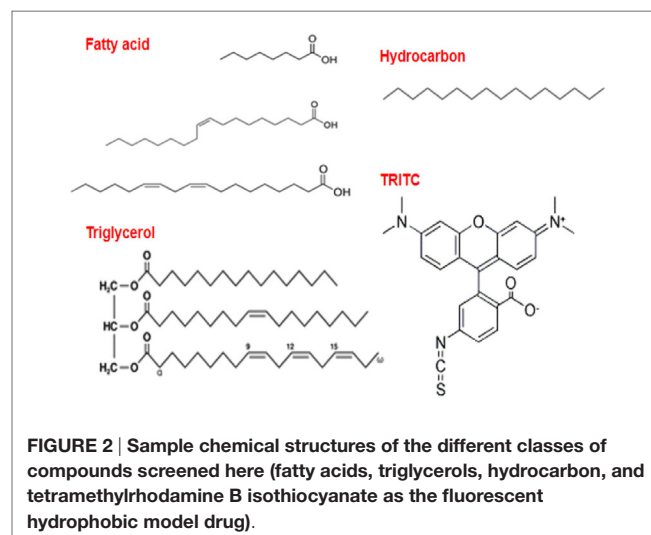


FIGURE 2 | Sample chemical structures of the different classes of compounds screened here (fatty acids, triglycerols, hydrocarbon, and tetramethylrhodamine B isothiocyanate as the fluorescent hydrophobic model drug).

TABLE 1 | List of components [the combinations have the ratio of 1:1 (w/w)].

1	Hexanoic acid only	43	Octanoic and sunflower	85	Peanut and cottonseed	127	Olive and hexadecane	169	Safflower and hexadecane
2	Hexanoic and octanoic	44	Octanoic and canola	86	Peanut and linseed	128	Olive and glycerol	170	Safflower and glycerol
3	Hexanoic and oleic	45	Octanoic and sesame	87	Peanut and safflower	129	Soybean oil only	171	Sunflower oil only
4	Hexanoic and linoleic	46	Octanoic and castor	88	Peanut and sunflower	130	Soybean and olive	172	Sunflower and canola
5	Hexanoic and soybean	47	Octanoic and fish	89	Peanut and canola	131	Soybean and peanut	173	Sunflower and sesame
6	Hexanoic and olive	48	Octanoic and mineral	90	Peanut and sesame	132	Soybean and corn	174	Sunflower and castor
7	Hexanoic and peanut	49	Octanoic and lavender	91	Peanut and castor	133	Soybean and sunflower	175	Sunflower and hexadecane
8	Hexanoic and corn	50	Octanoic and hexadecane	92	Peanut and fish	134	Soybean and cottonseed	176	Sunflower and fish
9	Hexanoic and cottonseed	51	Octanoic and glycerol	93	Peanut and mineral	135	Soybean and linseed	177	Sunflower and mineral
10	Hexanoic and linseed	52	Corn oil only	94	Peanut and lavender	136	Soybean and safflower	178	Sunflower and lavender
11	Hexanoic and safflower	53	Corn and cottonseed	95	Peanut and hexadecane	137	Soybean and canola	179	Sunflower and glycerol
12	Hexanoic and sunflower	54	Corn and linseed	96	Peanut and glycerol	138	Soybean and sesame	180	Canola oil only
13	Hexanoic and canola	55	Corn and safflower	97	Linoleic acid only	139	Soybean and castor	181	Canola and sesame
14	Hexanoic and sesame	56	Corn and sunflower	98	Linoleic and soybean	140	Soybean and fish	182	Canola and castor
15	Hexanoic and castor	57	Corn and canola	99	Linoleic and olive	141	Soybean and glycerol	183	Canola and hexadecane
16	Hexanoic and fish	58	Corn and sesame	100	Linoleic and peanut	142	Soybean and mineral	184	Canola and fish
17	Hexanoic and mineral	59	Corn and castor	101	Linoleic and corn	143	Soybean and lavender	185	Canola and mineral
18	Hexanoic and lavender	60	Corn and fish	102	Linoleic and cottonseed	144	Soybean and hexadecane	186	Canola and lavender
19	Hexanoic and hexadecane	61	Corn and mineral	103	Linoleic and linseed	145	Fish oil only	187	Canola and glycerol
20	Hexanoic and glycerol	62	Corn and lavender	104	Linoleic and safflower	146	Fish and mineral	188	Mineral oil only
21	Cottonseed oil only	63	Corn and hexadecane	105	Linoleic and sunflower	147	Fish and lavender	189	Mineral and lavender
22	Cottonseed and linseed	64	Corn and glycerol	106	Linoleic and canola	148	Fish and hexadecane	190	Mineral and hexadecane
23	Cottonseed and safflower	65	Oleic acid only	107	Linoleic and sesame	149	Fish and glycerol	191	Mineral and glycerol
24	Cottonseed and sunflower	66	Oleic and linoleic	108	Linoleic and castor	150	Linseed oil only	192	Sesame oil only
25	Cottonseed and canola	67	Oleic and soybean	109	Linoleic and fish	151	Linseed and safflower	193	Sesame and castor
26	Cottonseed and sesame	68	Oleic and olive	110	Linoleic and mineral	152	Linseed and sunflower	194	Sesame and fish
27	Cottonseed and castor	69	Oleic and peanut	111	Linoleic and lavender	153	Linseed and canola	195	Sesame and mineral
28	Cottonseed and fish	70	Oleic and corn	112	Linoleic and hexadecane	154	Linseed and mineral	196	Castor oil only
29	Cottonseed and mineral	71	Oleic and cottonseed	113	Linoleic and glycerol	155	Linseed and sesame	197	Sesame and Lavender
30	Cottonseed and lavender	72	Oleic and linseed	114	Olive oil only	156	Linseed and castor	198	Sesame and hexadecane
31	Cottonseed and hexadecane	73	Oleic and safflower	115	Olive and peanut	157	Linseed and fish	199	Sesame and glycerol
32	Cottonseed and glycerol	74	Oleic and sunflower	116	Olive and corn	158	Linseed and lavender	200	Castor and fish
33	Octanoic acid only	75	Oleic and canola	117	Olive and cottonseed	159	Linseed and hexadecane	201	Castor and mineral
34	Octanoic and oleic	76	Oleic and sesame	118	Olive and linseed	160	Linseed and glycerol	202	Castor and lavender
35	Octanoic and linoleic	77	Oleic and castor	119	Olive and safflower	161	Safflower oil only	203	Castor and hexadecane
36	Octanoic and soybean	78	Oleic and fish	120	Olive and sunflower	162	Safflower and castor	204	Lavender and glycerol
37	Octanoic and olive	79	Oleic and mineral	121	Olive and canola	163	Safflower and sunflower	205	Castor and glycerol
38	Octanoic and peanut	80	Oleic and lavender	122	Olive and sesame	164	Safflower and canola	206	Lavender oil only
39	Octanoic and corn	81	Oleic and hexadecane	123	Olive and castor	165	Safflower and sesame	207	Lavender and hexadecane
40	Octanoic and cottonseed	82	Oleic and glycerol	124	Olive and fish	166	Safflower and fish	208	Hexadecane only
41	Octanoic and linseed	83	Peanut oil only	125	Olive and mineral	167	Safflower and mineral	209	Hexadecane and glycerol
42	Octanoic and safflower	84	Peanut and corn	126	Olive and lavender	168	Safflower and lavender	210	Glycerol only

and tetramethylrhodamine B isothiocyanate (TRITC), as the fluorescent hydrophobic model drug, which are purchased from Sigma-Aldrich. The combinations of 1:1 (w/w) liquid lipids and the pure lipids are tested (Table 1). The oil phase must be of high purity and free of undesirable components such as peroxides, pigments, decomposition products, and unsaponifiable matter such as sterols and polymers. Oxidation of oil and drug during preparation and storage must be minimized by manufacturing under a nitrogen atmosphere, as reported by Floyd (1999).

PDMS Stamps

PDMS micro-well stamps are prepared from a thermoplastic master (EV Group, Inc., Tempe, AZ, USA) cured from a patterned silicon wafer with 5 μm diameter wells, 2.5 μm deep and 10 μm in pitch, covering 19% of the stamp surface. The silicon wafers are initially cleaned with piranha solution or plasma treated and

later passivated with a 0.2% (by volume) octadecyltrichlorosilane solution in toluene. The PDMS stamp of desired dimensions is prepared from a Sylgard 184 (Dow Corning, Midland, MI, USA) elastomer gel at a ratio of 1:10 curing agent to base prepolymer poured over the thermoplastic master and cured in an oven at 65°C overnight.

Ink Preparation

For integration of multiple inks, TRITC, as a model drug, is added to the liquid lipids at a proportion of 1% by mass for arraying, screening, and microscopy. The results are microarrayed in an array pattern onto a PDMS ink palette.

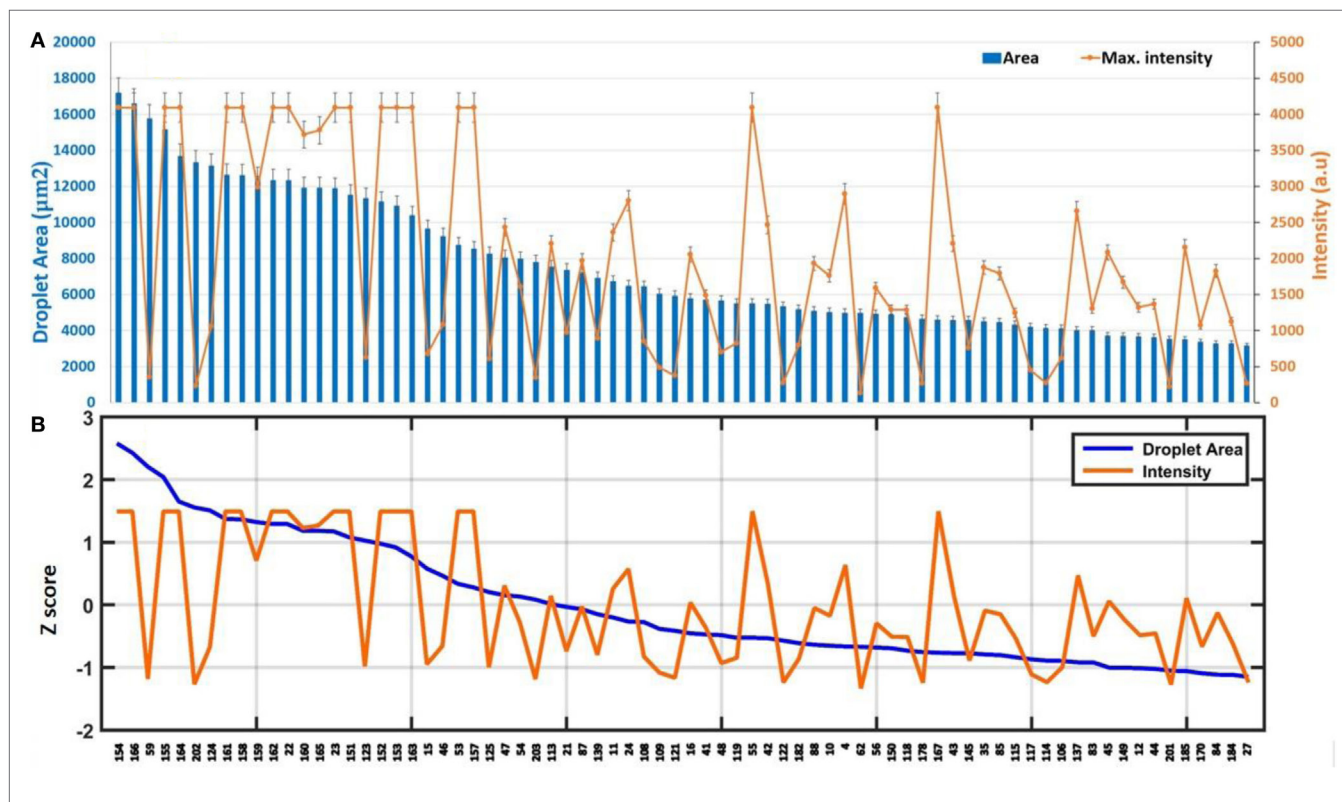
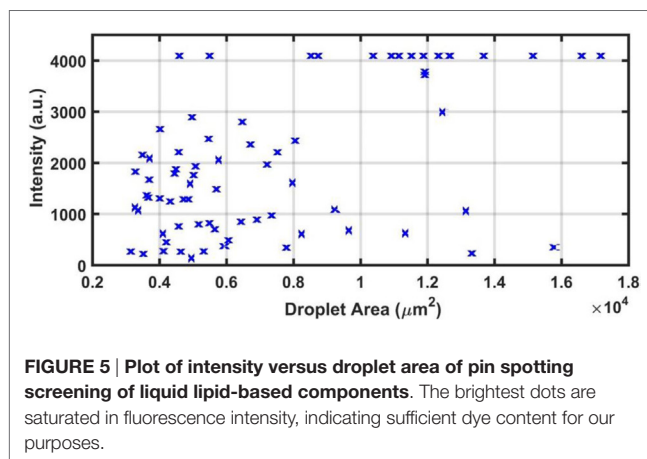
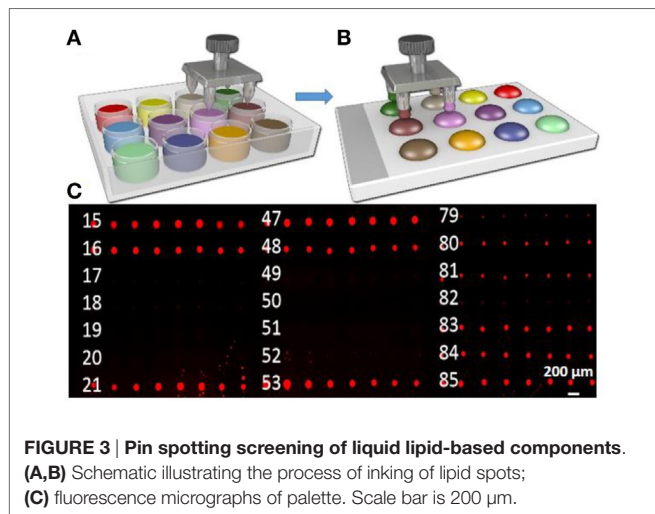
Microarraying Lipid Components

The different lipid solutions are microarrayed from standard 384-well microtiter plates (Axygen, Inc., PMI110-07 V1, Union

City, CA, USA) using a Microarrayer (Arrayit Corporation, ARYC) onto the PDMS palettes (Figure 3 and Figure S1 in Supplementary Material), using a 200 μm 4 \times 4 stainless steel microspot pin tool. Microarray pins are washed to ensure no cross-contamination between inks. It is found that 2 min washes in acetone and then water, followed by 30 sec of drying sufficed.

Intaglio Printing

For lipid/dye combination stamping on the cover glass palette surfaces, the PDMS stamp is inked and placed in contact with the substrate. A structured PDMS stamp is inked by pressing the patterned surface onto the ink palette (Lowry et al., 2014). The stamping procedure combines the topographical control of nano-imprint lithography and throughput of microcontact printing with the scalability of pin spotting. The stamps are left in direct contact with the surface and uniform, firm pressure (about 45 N



as measured on a bathroom scale) is applied for ~10 sec before careful removal and printing the next pattern. Excess material is removed by sacrificially printing four to six times before pattern

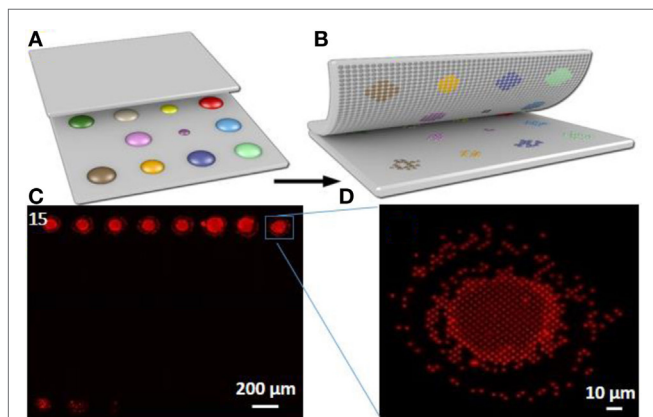


FIGURE 6 | Nanointaglio print compatibility screening of liquid lipid-based components in terms of area and intensity. (A,B) Schematic illustrating the process of nanointaglio printing of lipid spots; **(C)** fluorescence micrograph of a lipid microarray printed using the nanointaglio method; **(D)** magnified section of **(C)** indicated by blue square in **(C)**.

would print uniformly. Image analysis for area and intensity of the droplets is done by NIH ImageJ software (<http://rsb.info.nih.gov/ij/>) (**Figure 4A**; Figure S2 in Supplementary Material).

Quantitative analysis of pin spotting screening of liquid lipid-based components, together with the Z value of the components, is shown in **Figure 4**. Furthermore, a scatter plot of the two parameters tested (intensity and droplet area) is provided (**Figure 5**).

For **Figure 6** and Figure S3 in Supplementary Material, nanointaglio patterns are printed on glass coverslip substrates. Furthermore, quantitative analysis of the printing compatibility screening of liquid lipid-based components and their Z values are shown in **Figure 7**. The description of the correlation of intensity and print area is provided in **Figure 8**.

Lipid Nanopattern Storage and Immersion

After nanointaglio fabrication, lipid patterns are stored in a nitrogen glovebox (Mbraun, Inc., Model Labstar (1200/780), Stratham, NH, USA) to prevent them from possible oxidation. The nitrogen environment stabilizes the lipid nanostructures by dehydration prior to immersion in water (Lenhert et al., 2010). Then Millipore water is applied for 1 h, using a syringe directly over a section of the lipid pattern on a microscope stage while the pattern is being imaged on fluorescence microscope (**Figure 9**). Moreover,

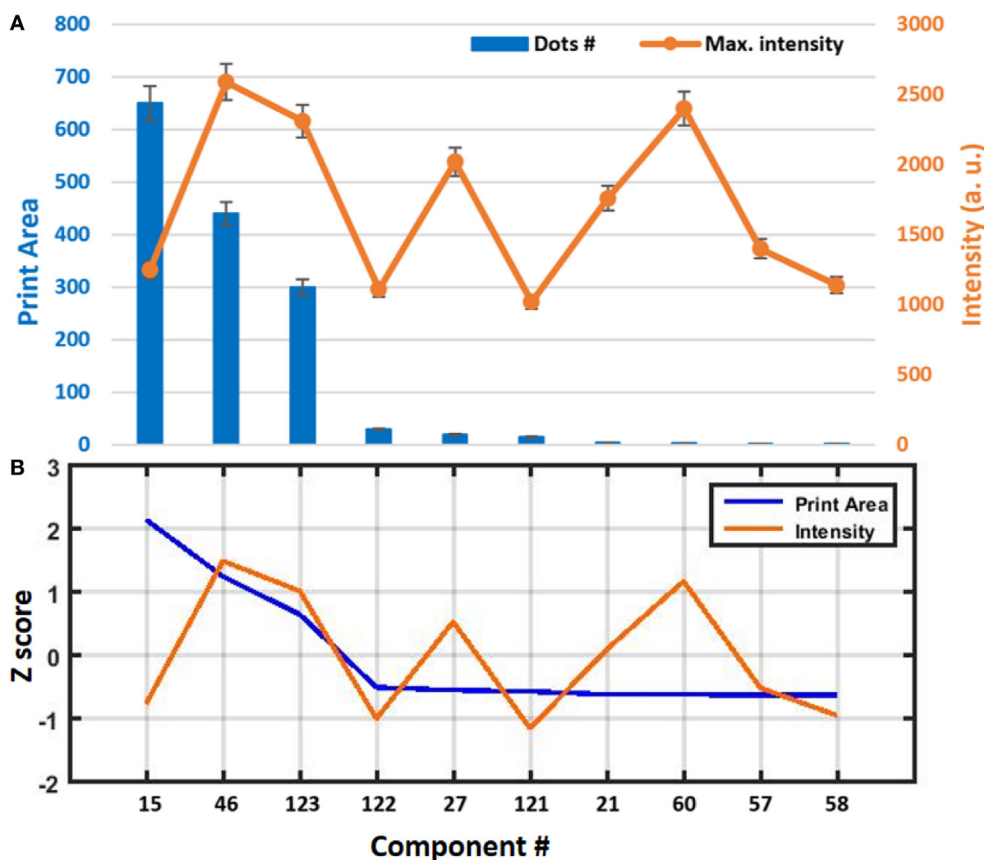
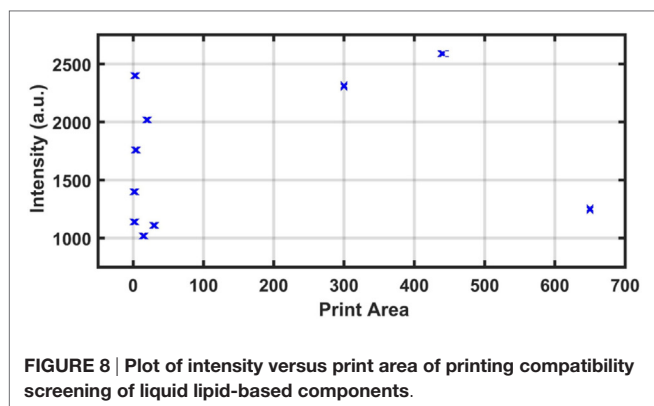


FIGURE 7 | (A) Quantitative analysis of the print compatibility screening of liquid lipid-based components in terms of print area and intensity. Error bars represent the SEM of at least nine different spots. **(B)** Z value of the components.



we repeat the same experiment for the selected components over a large pattern. This time after being imaged for 1 h, the patterns are kept at ambient temperature ($25^{\circ}\text{C} \pm 2\%$) for 72 h and are imaged again by fluorescence microscopy.

Preparation of Immersion Chamber

A 0.5 cm diameter cork bore is used to create cutouts in PDMS pieces 1 cm wide by 3 cm long by 0.5 cm thick. This chamber is placed on a glass slide with the lipid patterns to create an enclosed space to contain solution for experiments.

Characterization and Imaging Techniques

A Ti-E epifluorescence inverted microscope (Nikon Instruments, Melville, NY, USA) fitted with a Retiga SRV (QImaging, Canada) CCD camera (1.4 MP, Peltier cooled to -45°C) is used for fluorescence and bright-field imaging of the lipid patterns on glass surfaces. All experiments are performed at ambient temperature.

Statistical Analysis

All experiments are performed at least in triplicate. The screening data are repeated three times on three different days. Means and SEs of the means are calculated using Excel. MATLAB software is used to perform the Z score calculations. The raw intensity and droplet area data for each experiment are used for the calculation of Z scores. Z scores are calculated by subtracting the overall average of either intensity or droplet area (within a single experiment) from the raw intensity or droplet area data for each component and dividing that result by the SD of all the measured intensities or droplet areas, according to the formula:

$$Z \text{ score} = \left(\text{intensity}_c - \text{mean intensity}_{C1 \dots Cn} \right) / \text{SD}_{C1 \dots Cn}$$

where C is any component on the microarray and $C1 \dots Cn$ represent the aggregate measure of all of the components.

RESULTS AND DISCUSSION

Lipids (long-chain triglycerols—LCTs and medium-chain triglycerols—MCTs) approved by the regulatory agencies, alone or in combination, are generally first choice for developing drug carrier formulations (Marten et al., 2006; Hippalgaonkar

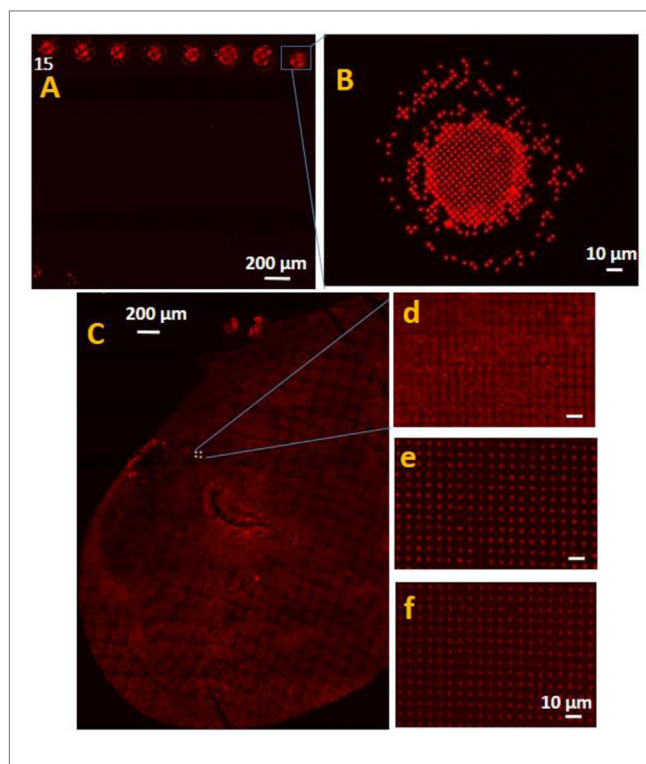


FIGURE 9 | The effect of immersion under water on liquid lipid stability of the samples stored under nitrogen atmosphere. (A) Fluorescence micrographs of castor oil/hexanoic acid combination in lipid microarray format 1 h after immersion under water and **(B)** magnified section of **(A)**. **(C)** Fluorescence micrograph of a large spot of castor oil/hexanoic acid combination printed using the nanointaglio method, **(D)** magnified section of **(C)** indicated by blue square in **(C)**; **(E)** fluorescence micrographs of the same spot after 1 h and **(F)** after 72 h immersion under water.

et al., 2010). LCTs such as soybean oil, safflower oil, sesame oil, and castor oil are approved for clinical use. Some oils (e.g., safflower, olive, sunflower, and castor) that contain more than 70% of oleic, linoleic, or ricinoleic acids make the larger spots. Our microarray includes both LCTs and MCTs and their combinations. Some oils such as linseed, safflower, and olive oils have higher fluorescence intensity, which is attributed to their autofluorescence properties (Sikorska et al., 2012). It is worth mentioning that the maximum fluorescence intensity of each spot is used in analyzing the data. Also, area values that are smaller than $3000 \mu\text{m}^2$ have not been considered.

In the fluorescence micrograph of the palette presented in **Figure 3** (Figure S1 in Supplementary Material), it is evident that not all the lipid mixtures are compatible with the pin-spotting step. Some of the components have not been pin spotted properly, as they show no fluorescence intensity. In addition, some of the samples have covered very limited area, which is almost negligible. In **Figure 4B**, Z scores provide a relative, semiquantitative estimate of either intensity or droplet area levels and, as such, form the basis of comparison of either intensity or droplet area data among many experiments within the same array type. Thus, Z scores provide a useful and intuitive method for visualizing and interpreting very large amounts of data in their natural physico-chemical context. This is in contrast to normalization strategies

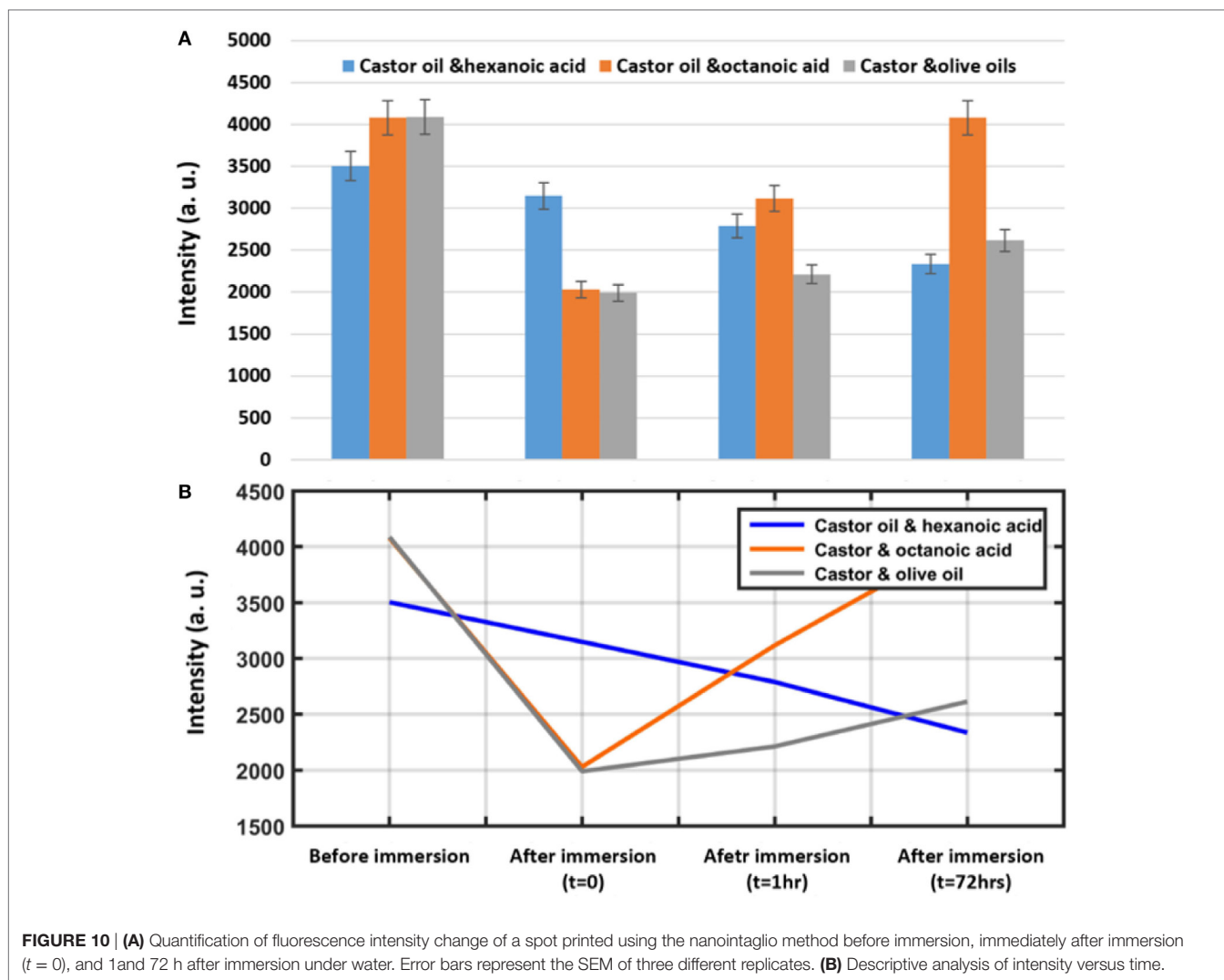


FIGURE 10 | (A) Quantification of fluorescence intensity change of a spot printed using the nanointaglio method before immersion, immediately after immersion ($t = 0$), and 1 and 72 h after immersion under water. Error bars represent the SEM of three different replicates. **(B)** Descriptive analysis of intensity versus time.

that express either intensity or droplet area data as ratios of one sample to another (either experimental or to a common reference sample). Positive and negative values in these analyses simply indicate their relationship to the normalizing sample rather than reflecting actual area or intensity levels. The very brightest dots are saturated, indicating that a sufficiently large amount of dye per dot as fluorescence intensity is related to droplet height (Nafday and Lenhert, 2011). Droplet area is likely related to both droplet volume and the contact angle of the oil on the glass surface. The viscosity of the oil and contact time of the tip may also play a role in the lipid transfer from the pin to the surface.

Castor oil, which contains monounsaturated fatty acyls, shows the most stable formulation after immersion, especially when combined with other components. Vegetable oils contain various triglycerides in different proportions; castor oil, in particular, deviates from the other oils by the high content of a monounsaturated fatty acid [ricoleic acid, 18:19 (12OH)] with a hydroxy group. For example, the free fatty acids contained in castor oil can act as a coemulsifier resulting in lower interfacial tension and more stable formulation in comparison with the other oil phases

(Mohan et al., 2012). Compared to other vegetable oils, castor oil exhibits enhanced solubilizing effects that can be ascribed to increased hydrogen bonding activities of the hydroxyl groups in ricinoleic acids.

Furthermore, it has been shown that by combining castor oil and a liquid fatty acid, at the ratio of 1:1 (w/w), the stability of the material under water is increased. Jumaa and Muller (1998, 1999) reported the effect of mixing castor oil with medium chain triglycerides on the viscosity of castor oil. The oil combination, at the ratio of 1:1 (w/w), led to a decrease in the viscosity of castor oil and simultaneously to a decrease in the interfacial tension of the oil phase (Mohan et al., 2012). This was related to the free fatty acids contained in castor oil, which can act as a coemulsifier resulting in lower interfacial tension and, simultaneously, in a more stable formulation in comparison with the other oil phases.

In our microarray, castor oil/hexanoic acid (MCT), castor oil/octanoic acid (MCT), and castor oil/olive oil (LCT) combinations make small patterns after pin spotting with almost uniform light intensity distribution throughout the sample, and they make good printed patterns that are reproducible. As shown in **Figure 9**, for

castor oil/hexanoic acid combination, an irregular pattern of droplets is formed.

The dots are stable after immersion under water for 1 h in terms of the size, which demonstrates that the dots are not spreading; however, their intensity decreased during the time. As shown in **Figure 10A**, castor oil/octanoic acid combination shows almost complete fluorescence recovery 72 h after immersion under water. Intensities shown in **Figure 10** represent the average of 30 different areas measured on three different replicate samples (10 images each). The castor/olive oil combination shows a lower fluorescence recovery compared to the castor oil/octanoic acid combination. However, the castor oil/hexanoic acid combination shows a continuous decrease in fluorescence during that time. The latter finding may suggest a mixture more prone to TRITC (and maybe drug) release over time in aqueous solutions.

Both castor oil and MCTs (hexanoic acid) are among the excipients that are being used for the manufacturing of ocular compatible lipid emulsion (Mohan et al., 2012). However, prior to the formulation of the lipid emulsions, data are needed concerning drug solubility in the oil vehicle. In addition, information is needed on compatibility of the oil vehicle with other formulation additives and with the established ocular tissue, before the dosage forms can be prepared. Our results indicate that microdroplet arrays of castor oil combinations on surfaces are suitable for screening of drugs in a scalable manner.

CONCLUSION

A screen was carried out to identify oils compatible with pin spotting and nanointaglio, followed by immersion of the microarray into water. We tested 210 lipid formulations, and a 1:1 mixture of castor oil and hexanoic acid was found to be optimal in terms of droplet size, reproducibility of printed patterns, fluorescence intensity, and stability under immersion. Compared to

phospholipid carriers (Kusi-Appiah et al., 2015), this formulation can be arrayed without the need for an additional solvent. The lipid itself can be considered the solvent for the fabrication of drug screening microarrays. These “solvent-free” lipid multilayer microarrays have potential for HTS of lipophilic compounds.

AUTHOR CONTRIBUTIONS

LG carried out the experiments and wrote the manuscript together with SL. SL conceived of the study and directed the experiments.

ACKNOWLEDGMENTS

LG would like to thank Aubrey Kusi-Appiah at the Florida State University for helpful discussions. The authors thank Jen Kennedy for proofreading.

FUNDING

This work was supported by NIH R01 GM107172.

SUPPLEMENTARY MATERIAL

The Supplementary Material for this article can be found online at <http://journal.frontiersin.org/article/10.3389/fmats.2016.00055/full#supplementary-material>.

FIGURE S1 | Fluorescence micrograph of liquid lipid-based components pin spotted on PDMS palette. Scale bar is 200 μm .

FIGURE S2 | Fluorescence micrograph of a liquid lipid-based microarray printed using the nanointaglio method.

FIGURE S3 | Fluorescence micrograph of the liquid lipid-based microarray 1 h after immersion under water, which shows the effect of immersion under water on samples stability.

REFERENCES

- Anna, S. L., Bontoux, N., and Stone, H. A. (2003). Formation of dispersions using “flow focusing” in microchannels. *Appl. Phys. Lett.* 82, 364–366. doi:10.1063/1.1537519
- Arrabito, G., Galati, C., Castellano, S., and Pignataro, B. (2013). Luminometric sub-nanoliter droplet-to-droplet array (LUMDA) and its application to drug screening by phase I metabolism enzymes. *Lab. Chip* 13, 68–72. doi:10.1039/c2lc40948h
- Bailey, S. N., Sabatini, D. M., and Stockwell, B. R. (2004). Microarrays of small molecules embedded in biodegradable polymers for use in mammalian cell-based screens. *Proc. Natl. Acad. Sci. U.S.A.* 101, 16144–16149. doi:10.1073/pnas.0404425101
- Cahill, D. J. (2001). Protein and antibody arrays and their medical applications. *J. Immunol. Methods* 250, 81–91. doi:10.1016/S0022-1759(01)00325-8
- Comley, J. (2006). “Tools and technologies that facilitate automated screening” in *High-Throughput Screening in Drug Discovery*, ed. J. Hueser (Weinheim: Wiley-VCH), 37–73.
- Floyd, A. G. (1999). Top ten considerations in the development of parenteral emulsions. *Pharm. Sci. Technol. Today* 2, 134–143. doi:10.1016/S1461-5347(99)00141-8
- Gosalia, D. N., and Diamond, S. L. (2003). Printing chemical libraries on microarrays for fluid phase nanoliter reactions. *Proc. Natl. Acad. Sci. U.S.A.* 100, 8721–8726. doi:10.1073/pnas.1530261100
- Heller, M. J. (2002). DNA microarray technology: devices, systems, and applications. *Annu. Rev. Biomed. Eng.* 4, 129–153. doi:10.1146/annurev.bioeng.4.020702.153438
- Hippalgaonkar, K., Majumdar, S., and Kansara, V. (2010). Injectable lipid emulsions – advancements, opportunities and challenges. *AAPS PharmSciTech* 11, 1526–1540. doi:10.1208/s12249-010-9526-5
- Hirtz, M., Sekula-Neuner, S., Urtizberea, A., and Fuchs, H. (2015). “Functional lipid assemblies by dip-pen nanolithography and polymer pen lithography,” in *Soft Matter Nanotechnology: From Structure to Function*, eds X.Chen and H.Fuchs (Weinheim: Wiley-VCH), 161–185.
- Hong, J., Edel, J. B., and deMello, A. J. (2009). Micro- and nanofluidic systems for high-throughput biological screening. *Drug Discov. Today* 14, 134–146. doi:10.1016/j.drudis.2008.10.001
- Hook, A. L., Thissen, H., and Voelcker, N. H. (2006). Surface manipulation of biomolecules for cell microarray applications. *Trends Biotechnol.* 24, 471–477. doi:10.1016/j.tibtech.2006.08.001
- Howbrook, D. N., van der Valk, A. M., O’Shaughnessy, M. C., Sarker, D. K., Baker, S. C., and Lloyd, A. W. (2003). Developments in microarray technologies. *Drug Discov. Today* 8, 642–651. doi:10.1016/S1359-6446(03)02773-9
- Jumaa, M., and Muller, B. W. (1998). The effect of oil components and homogenization condition on the physicochemical properties and stability of parenteral fat emulsions. *Int. J. Pharm.* 163, 81–89. doi:10.1016/S0378-5173(97)00369-4
- Jumaa, M., and Muller, B. W. (1999). Physicochemical properties of chitosan-lipid emulsions and their stability during the autoclaving process. *Int. J. Pharm.* 183, 175–184. doi:10.1016/S0378-5173(99)00086-1
- Kalepu, S., and Nekkanti, V. (2015). Insoluble drug delivery strategies: review of recent advances and business prospects. *Acta Pharm. Sin. B* 5, 442–453. doi:10.1016/j.apsb.2015.07.003

- Kim, M., Pan, M., Gai, Y., Pang, S., Han, C., Yang, C., et al. (2015). Optofluidic ultrahigh-throughput detection of fluorescent drops. *Lab. Chip* 15, 1417–1423. doi:10.1039/c4lc01465k
- Kusi-Appiah, A. E., Lowry, T. W., Darrow, E. M., Wilson, K. A., Chadwick, B. P., Davidson, M. W., et al. (2015). Quantitative dose-response curves from subcellular lipid multilayer microarrays. *Lab. Chip* 15, 3397–3404. doi:10.1039/c5lc00478k
- Kusi-Appiah, A. E., Vafai, N., Cranfill, P. J., Davidson, M. W., and Lenhert, S. (2012). Lipid multilayer microarrays for in vitro liposomal drug delivery and screening. *Biomaterials* 33, 4187–4194. doi:10.1016/j.biomaterials.2012.02.023
- Lenhert, S., Brinkmann, F., Laue, T., Walheim, S., Vannahme, C., Klinkhammer, S., et al. (2010). Lipid multilayer gratings. *Nat. Nanotechnol.* 5, 275–279. doi:10.1038/nnano.2010.17
- Lenhert, S., Sun, P., Wang, Y., Fuchs, H., and Mirkin, C. A. (2007). Massively parallel dip-pen nanolithography of heterogeneous supported phospholipid multilayer patterns. *Small* 3, 71–75. doi:10.1002/smll.200600431
- Lowry, T. W., Kusi-Appiah, A., Guan, J., Van Winkle, D. H., Davidson, M. W., and Lenhert, S. (2014). Materials Integration by nanointaglio. *Adv. Mater. Interfaces* 1, 1300121–1300125. doi:10.1002/admi.201300127
- Ma, H., and Horiuchi, K. Y. (2006). Chemical microarray: a new tool for drug screening and discovery. *Drug Discov. Today* 11, 661–668. doi:10.1016/j.drudis.2006.05.002
- Marten, B., Pfeuffer, M., and Schrezenmeir, J. (2006). Medium-chain triglycerides. *Int. Dairy J.* 16, 1374–1382. doi:10.1016/j.idairyj.2006.06.015
- Mohan, K., Pravin, S., and Atul, B. (2012). Ophthalmic microemulsion: a comprehensive review. *Int. J. Pharma. Bio. Sci.* 3, 1–13.
- Mugherli, L., Burchak, O. N., Balakireva, L. A., Thomas, A., Chatelain, F., and Balakirev, M. Y. (2009). In situ assembly and screening of enzyme inhibitors with surface-tension microarrays. *Angew. Chem. Int. Ed.* 121, 7775–7780. doi:10.1002/ange.200901139
- Nafday, O. A., and Lenhert, S. (2011). High-throughput optical quality control of lipid multilayers fabricated by dip-pen nanolithography. *Nanotechnology* 22, 225301. doi:10.1088/0957-4484/22/22/225301
- Nafday, O. A., Lowry, T. W., and Lenhert, S. (2012). Multifunctional lipid multilayer stamping. *Small* 8, 1021–1028. doi:10.1002/smll.201102096
- Pirrung, M. C. (2002). How to make a DNA chip. *Angew. Chem. Int. Ed.* 41, 1276–1289. doi:10.1002/1521-3773(20020415)41:8<1276::AID-ANIE1276>3.0.CO;2-2
- Popova, A. A., Demir, K., Hartanto, T. G., Schmitta, E., and Levkin, P. A. (2016). Droplet-microarray on superhydrophobic-superhydrophilic patterns for high-throughput live cell screenings. *RSC Adv.* 6, 38263–38276. doi:10.1039/C6RA06011K
- Rohrer, H. (1996). The nanoworld: chances and challenges. *Microelectron. Eng.* 32, 5–14. doi:10.1016/0167-9317(95)00173-5
- Sikorska, E., Khmelinskii, I., and Sikorski, M. (2012). “Analysis of olive oils by fluorescence spectroscopy: methods and applications,” in *Olive Oil – Constituents, Quality, Health Properties and Bioconversions*, ed. D. Boskou (InTech). Available at: <http://www.intechopen.com/books/olive-oil-constituents-quality-health-properties-and-bioconversions/analysis-of-olive-oils-by-fluorescence-spectroscopy-methods-and-applications>
- Sun, Y., Chen, X., Zhou, X., Zhu, J., and Yu, Y. (2015). Droplet-in-oil array for picoliter-scale analysis based on sequential inkjet printing. *Lab. Chip* 15, 2429–2436. doi:10.1039/c5lc00356c
- Vafai, N., Lowry, T. W., Wilson, K. A., Davidson, M. W., and Lenhert, S. (2015). Evaporative edge lithography of a liposomal drug microarray for cell migration assays. *Nanofabrication* 2, 32–42. doi:10.1515/nanofab-2015-0004
- Wu, J., Wheeldon, I., Guo, Y., Lu, T., Du, Y., Wang, B., et al. (2011). A sandwiched microarray platform for benchtop cell-based high throughput screening. *Biomaterials* 32, 841–848. doi:10.1016/j.biomaterials.2010.09.026

Conflict of Interest Statement: The authors declare that the research was conducted in the absence of any commercial or financial relationships that could be construed as a potential conflict of interest.

Copyright © 2016 Ghazanfari and Lenhert. This is an open-access article distributed under the terms of the Creative Commons Attribution License (CC BY). The use, distribution or reproduction in other forums is permitted, provided the original author(s) or licensor are credited and that the original publication in this journal is cited, in accordance with accepted academic practice. No use, distribution or reproduction is permitted which does not comply with these terms.